

A simple and rapid method for identification of lesions at high risk for the no-reflow phenomenon immediately before elective coronary stent implantation

Akira Suda^{1,4} · Shigeto Namiuchi¹  · Tomohiro Kawaguchi² · Taro Nihei³ · Toru Takii¹ · Kenya Saji¹ · Tadashi Sugie¹ · Atsushi Kato¹ · Hiroaki Shimokawa⁴

Received: 23 June 2015 / Accepted: 19 February 2016 / Published online: 2 March 2016
© Springer Japan 2016

Abstract We aimed to design a rapid and reliable method to identify coronary lesions at high risk for the no-reflow phenomenon before elective coronary stent implantation using integrated backscatter intravascular ultrasound (IB-IVUS). The no-reflow phenomenon occurring during elective percutaneous coronary intervention (PCI) worsens patient prognosis, regardless of whether the phenomenon is transient or persistent. We retrospectively studied 353 coronary lesions to identify factors potentially promoting the no-reflow phenomenon, including lesion location and severity. We also performed component analysis by two- and three-dimensional IB-IVUS before elective stent implantation. The cutoff values of the true lipid volume and estimated lipid volume (lipid area at the minimal lumen diameter site \times total stent length) for the no-reflow phenomenon were determined by receiver operating curve analysis. Type C lesions, regardless of location and a thrombolysis in myocardial flow grade of 0, were risk factors for the no-reflow phenomenon during PCI. The estimated lipid volume was significantly correlated with the true lipid volume ($R^2 = 0.778$, $p < 0.0001$). The cutoff value of the estimated lipid volume for the no-reflow phenomenon was 132.6 mm^3 (area under the curve = 0.719),

and the predictive value was equivalent to that of the true lipid volume. Lesions with an estimated lipid volume of $\geq 132.6 \text{ mm}^3$ had a significantly higher risk of the no-reflow phenomenon during elective stent implantation (odds ratio, 4.35; 95 % confidence interval, 1.67–12.7; $p = 0.0024$). The simple and rapid measurement of the estimated lipid volume immediately before stenting during PCI constitutes a reliable predictor of lesions at high risk for the no-reflow phenomenon.

Keywords Elective percutaneous coronary intervention · Lipid-rich plaque · Integrated backscatter intravascular ultrasound · No-reflow phenomenon

Introduction

The angiographic no-reflow phenomenon is a serious complication of percutaneous coronary intervention (PCI). It is defined as substantial coronary flow reduction despite successful dilation of an epicardial coronary artery [thrombolysis in myocardial infarction (TIMI) flow grade of <3]. The no-reflow phenomenon is strongly associated with adverse clinical outcomes, regardless of whether the phenomenon is transient or persistent [1–5]. No-reflow during PCI causes inadequate myocardial perfusion and unexpected myocardial infarction (MI). Although there are several causes of the no-reflow phenomenon (lipid leakage from atherosclerotic plaques, microvascular spasm, and thrombus formation), most cases of PCI-related no-reflow without infarction are triggered by distal microembolization [6].

The no-reflow phenomenon occurs in >20 % of patients undergoing primary PCI for acute MI and <2 % of patients undergoing elective PCI [7, 8]. Although rare, occurrence of the no-reflow phenomenon during elective PCI may

✉ Shigeto Namiuchi
nami@openhp.or.jp

¹ Department of Cardiology, Sendai City Medical Center, 5-22-1 Tsurugaya, Miyagino-ku, Sendai 983-0824, Japan

² Department of Cardiology, Tsuyama Chuo Hospital, Tsuyama, Japan

³ Department of Cardiology, Iwaki Kyoritsu General Hospital, Iwaki, Japan

⁴ Present Address: Department of Cardiovascular Medicine, Tohoku University, Sendai, Japan

precipitate unexpected MI and loss of cardiac function, both of which are serious adverse events. The identification of lesions at high risk of the no-reflow phenomenon prior to PCI is highly desirable to reduce the risk of no-reflow and its consequences.

Intravascular ultrasound (IVUS) is widely used to assess the target plaque and design a safe and efficient PCI strategy. Integrated backscatter IVUS (IB-IVUS) allows for analysis of the plaque components [9–14]. In acute coronary syndrome, lipid-rich plaques visualized with IVUS correlate positively with the no-reflow phenomenon [15–17]. The identification of high-risk lesions just before the stenting procedure could reduce the risk of the no-reflow phenomenon through use of embolic protection devices. The true lipid volume of the target plaque is accurately measured by three-dimensional (3D) IB-IVUS, but this is time consuming and impractical during PCI. Our study offers a rapid, simple method with which to identify high-risk lesions immediately before stenting based on the estimated lipid volume [lipid area at the minimal lumen diameter (MLD) site \times total stent length]. We provide cutoff values for both parameters and compare their reliability for the identification of coronary lesions at high risk for the post-stenting no-reflow phenomenon.

Materials and methods

Study population and lesion characteristics

We conducted a retrospective study of patients with atherosclerotic lesions who underwent elective coronary stent implantation without embolic protection devices at our institution from July 2010 to March 2013. The exclusion parameters were procedures without IB-IVUS before stenting, procedures without IB-IVUS due to the inability to cross the lesion with the IVUS catheter, and inadequate IB-IVUS images owing to extensive calcification.

Data collection

We analyzed baseline patient characteristics documented before admission for PCI, including age, sex, coronary risk factors, and medications. Lesion characteristics were analyzed, including target vessel (left main trunk, left anterior descending artery, left circumflex artery, and right coronary artery), lesion classification (Type A, B1, B2, and C), and the existence of a thrombus in the lesion. A thrombus at the target lesion was diagnosed angiographically as PCI began. The creatine kinase (CK) concentration was measured the day after PCI.

No-reflow phenomenon

No-reflow phenomenon is defined as coronary flow reduction following stent implantation and during the PCI procedure, despite successful dilation of the target coronary artery (TIMI flow grade of <3). All cases of no-reflow were identified angiographically. IVUS was used to confirm that no other factors causing coronary flow reduction were present, such as major dissection, hematoma, or a rich thrombus in the target lesion. All cases of no-reflow during PCI were recorded regardless of whether they were temporary or continuous at the end of the procedure.

Conventional IVUS analysis

Intravascular ultrasound scans were performed using a mechanical sector scanner (View It; Terumo Medical Corporation, Tokyo, Japan) and a motorized transducer pull-back system (0.5 mm/s). All patients received intravenous heparin (8000–10,000 U) and injection of isosorbide dinitrate (1.0–2.5 mg) or nicorandil (1.0–2.0 mg) into the target coronary artery before the procedure. A 6- to 8-French coronary guiding catheter and a 0.014-inch guidewire were used for IVUS catheter insertion into the target coronary artery. Quantitative measurements using IVUS were conducted as previously described [18]. The proximal reference site was defined as the site with the largest lumen proximal to a stenosis, but within the same segment. Similarly, the distal reference site was defined as the site with the largest lumen distal to a stenosis, but within the same segment. Lesion length was defined as the distance between the distal and proximal reference sites. The cross-sectional area (CSA) of the external elastic membrane (EEM) and lumen were measured on each slice (Fig. 1). The CSA of the atheroma (plaque + media) was calculated using these values (EEM CSA – lumen CSA). This measurement was conducted throughout the entire length of each target plaque at 1-mm intervals. Vessel and plaque volumes were calculated by integration of each CSA at 1-mm intervals. IVUS scans were conducted before coronary stent implantation. In lesions with grade 0 TIMI flow before PCI, we performed pre-dilation using a small-diameter balloon to assess the target lesion with IVUS.

IB-IVUS analysis

The IB values of each tissue component are expressed as the average power of the frequency component of the backscattered signal from a small volume of tissue, calculated using fast Fourier transformation and expressed in decibels. The image was divided into 512 vector lines (0.7

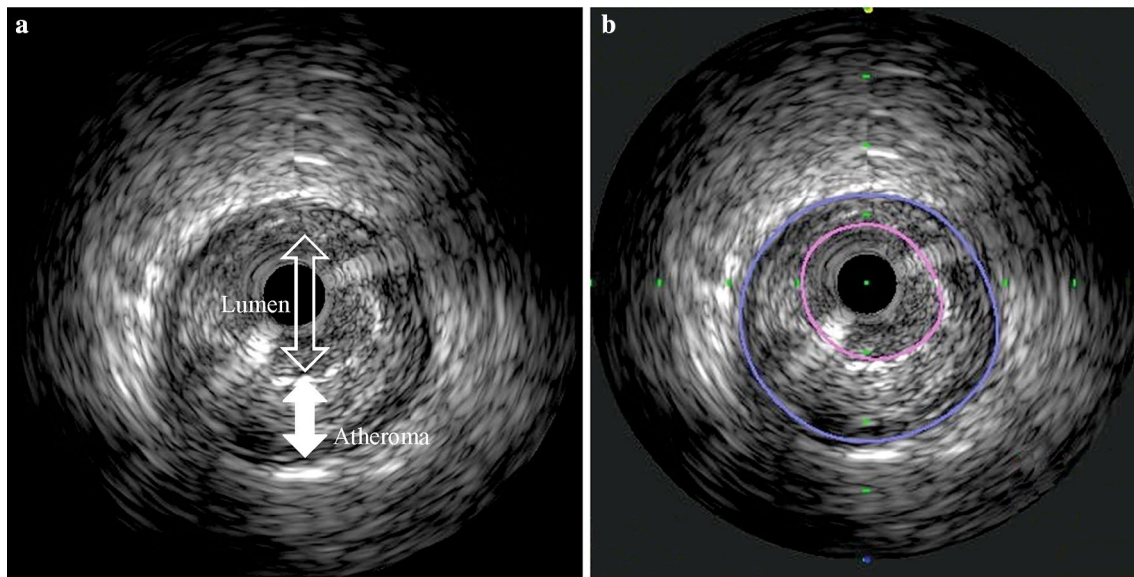


Fig. 1 Conventional intravascular ultrasound (IVUS) analysis of atheroma thickness. **a** Grayscale IVUS images of a coronary artery showing the cross-sectional area (CSA) of the atheroma (plaque + media) and the external elastic membrane (EEM) (*closed*

arrow atheroma, *open arrow* vessel lumen). **b** The analysis was conducted by tracing the external limit of the EEM-CSA (*purple line*) and lumen CSA (*pink line*) for each slice. The atheroma CSA was calculated as follows: EEM CSA – lumen CSA

grade per line), and 256 lesions of interest were defined at each 23.4- μ m depth on each vector line (total of 131,072 lesions of interest per image). The CSA of each atheroma was classified into four tissue types based on the range of IB values: lipid pool, $-73 < IB \leq -63$ decibels; fibrosis, $-63 < IB \leq -55$ decibels; dense fibrosis, $-54 < IB \leq -30$ decibels; and calcification, $-30 < IB \leq -23$ decibels (Fig. 2). A different color depicts each type of tissue: lipid (blue), fibrous (green), dense fibrous (yellow), and calcification (red). Three-dimensional IB-IVUS images were analyzed to calculate the volumes of the lipid pool, fibrosis, dense fibrosis, and calcification areas from the sum of each plaque CSA at 1-mm intervals.

True and estimated lipid volumes of target lesion

The lipid area of each slice was measured by IB-IVUS using the color-coded images, and the lipid volume was calculated by integration of each slice in the target lesion at 1-mm intervals. The true lipid volume was defined as the lipid volume of the target lesion. The estimated lipid volume of the target lesion was defined as the lipid area at the MLD site \times total stent length. The reliability of this parameter was determined by conducting correlation analyses between the true lipid volume and the estimated lipid volume of the target lesion. The cutoff values of both the true and estimated lipid volumes for development of the no-reflow phenomenon were calculated and compared by receiver operating characteristic (ROC) analysis.

Statistical analysis

The patients were separated into two groups: no-reflow negative (–) and no-reflow positive (+). Continuous data are presented as mean \pm standard deviation (or as median and interquartile range), and the groups were compared using Student's *t* test. Categorical data are presented as percentages, and the groups were compared by the Chi-square test. ROC analysis was performed to evaluate the cutoff values for no-reflow of the true lipid and estimated lipid volumes. To compare the prognostic accuracy of both measures for the development of the no-reflow phenomenon, logistic regression models were analyzed using three methods: discrimination measuring the area under the curve (AUC), calibration (Hosmer–Lemeshow test), and reclassification [net reclassification improvement (NRI) and integrated discrimination improvement (IDI)]. The AUC integrates the sensitivity and specificity of the variable with 1.00 representing a perfect predictive value and ≤ 0.50 being associated with chance. The Hosmer–Lemeshow test is an index of the goodness of fit for logistic regression models. If this test is not significant, the model has adequate fit for the data. The application of NRI and IDI provides the incremental value to AUC. These indices can detect the superiority or inferiority of the updated model directly by comparison with the initial model. Further, multivariate analysis was performed in two sets among the variables with an AUC of >0.70 for the development of the no-reflow phenomenon: one with

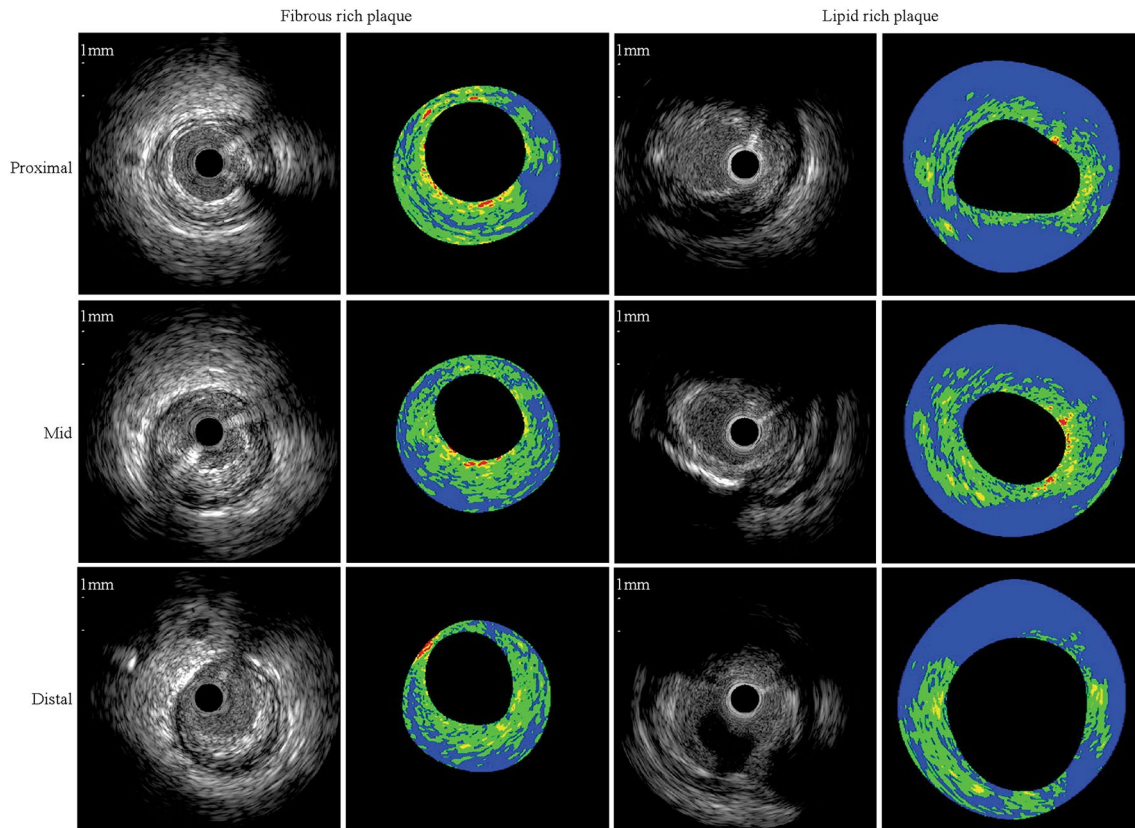


Fig. 2 Integrated backscatter intravascular ultrasound (IB-IVUS) imaging. Representative IB-IVUS images of a fibrous-rich plaque and lipid-rich plaque. The plaque + media cross-sectional area was

classified into four types of tissue according to differences in the IB values. *Color-coded* images demonstrate lipid (*blue*), fibrous (*green*), dens fibrous (*yellow*), and calcification (*red*)

the true lipid volume and the other with the estimated lipid volume. Values of $p < 0.05$ were considered statistically significant. Statistical analyses were conducted with JMP software (JMP version 9.0.2; SAS Institute, Cary, NC) and R software (<http://www.r-project.org/>).

Results

Patient characteristics and laboratory findings

During the enrollment period, coronary stents were implanted in a total of 504 lesions of 411 patients visiting our institute. We excluded all procedures without IB-IVUS imaging (41 lesions), those without IB-IVUS imaging performed before stent implantation because of the inability of the IVUS catheter to cross the target lesion (45 lesions), and those without analyzable IVUS images due to severe calcification (65 lesions). The remaining study population comprised 353 target lesions (70.0 %) of 252 patients (175 patients with 1 lesion and 77 patients with ≥ 2 lesions), assessed by IB-IVUS before the stent procedure. The no-reflow phenomenon developed in 19 lesions (5.4 %) after

stent implantation. IVUS images were acquired for 70.0 % of all lesions.

Table 1 compares the clinical characteristics and laboratory findings of the no-reflow (+) and no-reflow (−) groups. The no-reflow phenomenon was associated with relatively low hemoglobin levels ($p = 0.076$). However, there were no significant differences in morbidity due to dyslipidemia or diabetes mellitus, previous MI, preadmission medications, or blood lipid composition.

Target lesion characteristics, PCI procedures, and IVUS findings

Lesion characteristics before the procedure had a profound impact on the risk of the no-reflow phenomenon after elective PCI stent implantation (Table 2). Both patient groups exhibited comparable distributions of the location of the target vessel and frequency of thrombus formation. Only two lesions in the no-reflow (−) group had thrombus formation with grade 2 TIMI flow. In contrast, no-reflow occurred predominantly in the most severe lesions (Type C), which represented 36 % of lesions in the no-reflow (+) group compared with 12 % of lesions in the no-reflow

Table 1 Patient characteristics and laboratory findings

	Overall cohort ($n = 252$)	No-reflow (+) ($n = 17$)	No-reflow (–) ($n = 235$)	p
Age (years)	69 ± 11	72 ± 11	69 ± 11	0.24
Male	203 (81 %)	14 (82 %)	189 (80 %)	0.85
Body mass index (kg/m ²)	24.7 ± 3.5	23.3 ± 4.2	24.8 ± 3.5	0.10
Clinical presentation				
Stable angina pectoris	183 (73 %)	12 (70 %)	171 (73 %)	0.95
Unstable angina pectoris	31 (12 %)	2 (12 %)	29 (12 %)	
Silent myocardial ischemia	38 (15 %)	3 (18 %)	35 (15 %)	
Dyslipidemia	158 (63 %)	11 (65 %)	147 (63 %)	0.86
Diabetes mellitus	105 (42 %)	9 (53 %)	96 (41 %)	0.33
Hypertension	194 (77 %)	13 (76 %)	181 (77 %)	0.96
Previous myocardial infarction	121 (48 %)	7 (41 %)	114 (49 %)	0.56
Previous CABG	26 (10 %)	0 (0 %)	26 (11 %)	0.15
Aspirin at the time of planning PCI	218 (87 %)	15 (88 %)	203 (86 %)	0.83
Aspirin before PCI	246 (98 %)	16 (94 %)	230 (98 %)	0.33
Calcium channel blocker	113 (45 %)	6 (35 %)	107 (46 %)	0.41
Nitrates	125 (50 %)	6 (35 %)	119 (51 %)	0.22
Statin	157 (62 %)	11 (65 %)	146 (62 %)	0.83
Hemoglobin (g/dL)	13.3 ± 2.0	12.5 ± 2.4	13.3 ± 1.9	0.076
Creatinine (mg/dL)	0.99 ± 0.89	1.00 ± 0.29	0.99 ± 0.92	0.97
C-reactive protein (mg/dL)	0.1 (0.1, 0.2)	0.1 (0.1, 0.2)	0.1 (0.1, 0.3)	0.98
LDL-cholesterol (mg/dL)	102 ± 36	95 ± 25	102 ± 37	0.47
HDL-cholesterol (mg/dL)	46 ± 17	50 ± 13	46 ± 17	0.32
Triglyceride (mg/dL)	135 ± 80	103 ± 46	138 ± 82	0.086
HbA1c (%)	6.1 ± 1.0	6.0 ± 0.9	6.1 ± 1.0	0.69

CABG coronary artery bypass grafting, PCI percutaneous coronary intervention, LDL low-density lipoprotein, HDL high-density lipoprotein, HbA1c hemoglobin A1c

(–) group ($p = 0.006$). Furthermore, the no-reflow (+) group had more lesions with grade 0 TIMI flow than did the no-reflow (–) group. This suggests that Type C lesions and those with grade 0 TIMI flow lesions are at particular risk of developing the no-reflow phenomenon after stent implantation, regardless of their location. Pre-dilation using a balloon was performed more commonly in procedures with no-reflow. The maximum inflation pressure tended to be lower in the no-reflow (+) group than in the no-reflow (–) group ($p = 0.061$), and the procedural duration was longer in the no-reflow (+) group than in the no-reflow (–) group ($p < 0.0001$). Glycoprotein IIb/IIIa inhibitors were not administered in any case.

The IVUS images acquired during PCI, before stent implantation, were analyzed using conventional volumetric gray-scale analysis at the MLD site (Table 2). The lesions in the no-reflow (+) group had a significantly larger EEM CSA (1.2-fold; $p = 0.02$) and atheroma CSA (1.3-fold; $p = 0.0073$) than did the lesions in the no-reflow (–) group. These data are consistent with the 3D IVUS analysis, which showed 1.5-fold larger vessel volumes ($p = 0.004$) and 1.7-fold higher plaque

volumes ($p < 0.0001$) for lesions of the no-reflow (+) group. In contrast, IVUS images did not identify the extent of fibrosis or calcification as determinants of the no-reflow phenomenon. However, the lesions in the no-reflow (+) group exhibited a 1.5-fold larger lipid area at the MLD site ($p = 0.0018$; 2D IVUS analysis) and a 2.0-fold larger lipid volume for the whole lesion (true lipid volume; $p < 0.0001$; 3D IVUS analysis) than did the lesions in the no-reflow (–) group. Furthermore, the estimated lipid volume was twofold larger in lesions with no-reflow ($p < 0.0001$). These findings identify lipid parameters as the most sensitive indicators of the no-reflow phenomenon.

The PCI procedures required longer stents for the no-reflow (+) group, consistent with the higher frequency of Type C lesions. In the no-reflow (–) group, stenting restored adequate flow in all lesions, as indicated by the grade 3 TIMI flow. In the no-reflow (+) group, however, grade 3 TIMI flow could not be accomplished in seven lesions (37 %). CK activity on the day following elective stent implantation was significantly higher in patients with the no-reflow phenomenon.

Table 2 Target lesion characteristics, PCI procedures and IVUS findings

	Overall cohort (<i>n</i> = 353)	No-reflow (+) (<i>n</i> = 19)	No-reflow (−) (<i>n</i> = 334)	<i>p</i>
Location (LMT/LAD/LCx/RCA)	7/121/102/123	0/8/4/7	7/113/98/116	0.75
Type of lesion (A/B1/B2/C)	177/77/51/48	4/6/2/7	173/71/49/41	0.0060
Thrombus formation	2 (0.6 %)	0 (0 %)	2 (0.6 %)	0.74
TIMI flow grade before PCI (0/1/2/3)	21/11/37/284	4/1/3/11	17/10/34/273	0.020
Rotational atherectomy	7 (2.0 %)	0 (0 %)	7 (2.1 %)	0.52
Pre-dilation using balloon	140 (39.7 %)	15 (79.0 %)	125 (37.4 %)	0.0003
Post-dilation using balloon (except for stent delivery balloon)	99 (28.0 %)	3 (15.8 %)	96 (28.7 %)	0.22
Max inflation pressure (atm)	14.0 ± 3.5	12.6 ± 3.5	14.1 ± 3.5	0.061
Procedural duration (min)	58 ± 27	82 ± 30	57 ± 26	<0.0001
ACT level immediately following procedure (s)	332 ± 104	317 ± 45	333 ± 107	0.52
IVUS 2-D analysis at MLD site				
EEM CSA (mm ²)	13.5 ± 5.6	16.4 ± 7.5	13.3 ± 5.5	0.020
Atheroma CSA (mm ²)	10.9 ± 5.2	14.0 ± 7.1	10.7 ± 5.1	0.0073
Lipid area (mm ²)	6.5 ± 4.3	9.5 ± 6.3	6.4 ± 4.1	0.0018
Fibrosis area (mm ²)	3.7 ± 2.0	3.9 ± 1.5	3.7 ± 2.1	0.66
Dense fibrosis area (mm ²)	0.5 ± 0.3	0.5 ± 0.3	0.5 ± 0.3	0.96
Calcification area (mm ²)	0.2 ± 0.2	0.1 ± 0.2	0.2 ± 0.2	0.50
IVUS 3-D analysis				
Vessel volume (mm ³)	279.3 ± 179.7	419.4 ± 239.3	271.3 ± 172.7	0.0004
Plaque volume (mm ³)	181.6 ± 136.8	304.3 ± 194.2	174.7 ± 129.7	<0.0001
True lipid volume (mm ³)	102.2 ± 85.9	192.7 ± 141.3	97.1 ± 79.0	<0.0001
Fibrosis volume (mm ³)	67.6 ± 55.1	97.8 ± 64.3	65.9 ± 54.1	0.014
Dense fibrosis volume (mm ³)	8.7 ± 7.2	10.7 ± 6.5	8.6 ± 7.2	0.21
Calcification volume (mm ³)	3.0 ± 3.3	3.1 ± 2.7	3.0 ± 3.4	0.92
Total stent length (mm)	20 ± 10	27 ± 14	20 ± 10	0.0019
Estimated lipid volume (mm ³)	132.1 ± 118.3	266.2 ± 242.4	124.4 ± 102.6	<0.0001
TIMI flow grade after PCI (0/1/2/3)	0/1/6/346	0/1/6/12	0/0/0/334	<0.0001
Creatine kinase before PCI (IU/L)	81 (59, 117)	99 (64, 126)	80 (58, 116)	0.051
Creatine kinase 24 h post PCI (IU/L)	62 (44, 89)	185 (49, 461)	62 (44, 83)	<0.0001

PCI percutaneous coronary intervention, IVUS intravascular ultrasound, LMT left main trunk, LAD left anterior descending artery, LCx left circumflex artery, RCA right coronary artery, TIMI thrombolysis in myocardial infarction, ACT activated clotting time, MLD minimal lumen diameter, EEM external elastic membrane, CSA cross-sectional area

ROC analyses for development of the no-reflow phenomenon and correlation between true and estimated lipid volumes

Table 3 shows the AUC values of the variables evaluated for their potential impact on the no-reflow phenomenon. Four variables had AUC values of >0.700: plaque volume (0.760), total stent length (0.713), true lipid volume (0.741), and estimated lipid volume (0.719). Multivariate analyses revealed that only lipid volumes were significant predictors for the development of the no-reflow phenomenon; both the true lipid volume ($p = 0.024$) and the estimated lipid volume ($p = 0.033$) (Table 4). ROC analyses identified similar cutoff values for the true lipid volume (117.0 mm³; AUC 0.741) and estimated lipid volume

(132.6 mm³; AUC 0.719) for development of the no-reflow phenomenon. Positive predictive values were 12.3 % for the true lipid volume and 10.5 % for the estimated lipid volume. Negative predictive values were 97.6 % for the true lipid volume and 97.4 % for the estimated lipid volume. There was a strongly significant correlation between the true lipid volume and the estimated lipid volume in the target plaque ($R^2 = 0.778$, $p < 0.0001$) (Fig. 3). There was no significant difference between prediction of the no-reflow phenomenon using the true lipid volume or estimated lipid volume ($p = 0.21$) (Fig. 3).

The Hosmer–Lemeshow test was applied to determine the goodness of fit of the logistic regression model of the no-reflow phenomenon. The associated p value was 0.59, indicating no rejection of a good fit. Reclassification

Table 3 Receiver operating characteristic curve analysis of the associations between patient baseline characteristics or lesion characteristics and no-reflow after elective coronary stent implantation

Variable	AUC (95 % CI)	Sensitivity (%)	Specificity (%)
Age (years)	0.597 (0.451–0.743)	68.4	52.4
Dyslipidemia	0.508 (0.398–0.619)	68.4	33.2
Diabetes mellitus	0.551 (0.432–0.669)	52.6	57.5
Previous myocardial infarction	0.540 (0.422–0.657)	57.9	50.0
Aspirin	0.501 (0.415–0.588)	15.8	84.4
Calcium channel blocker	0.540 (0.426–0.655)	63.2	44.9
Nitrates	0.601 (0.490–0.712)	68.4	51.8
Statin	0.516 (0.405–0.626)	68.4	34.7
Hemoglobin (g/dL)	0.646 (0.492–0.799)	63.2	65.6
LDL-cholesterol (mg/dL)	0.544 (0.416–0.672)	52.6	65.3
Type C lesion	0.623 (0.510–0.736)	36.8	87.7
TIMI flow grade 0 before PCI	0.580 (0.485–0.675)	21.1	94.9
Lipid CSA (mm ²)	0.647 (0.502–0.791)	52.6	77.5
Total stent length (mm)	0.713 (0.605–0.820)	68.4	66.2
Plaque volume (mm ³)	0.760 (0.656–0.864)	78.9	65.0
True lipid volume (mm ³)	0.741 (0.616–0.865)	68.4	72.2
Estimated lipid volume (mm ³)	0.719 (0.590–0.848)	68.4	66.8

AUC area under the curve, CI confidence interval, CSA cross-section area, LDL low-density lipoproteins, TIMI thrombolysis in myocardial infarction

Table 4 Univariate and multivariate analysis for the development of no-reflow phenomenon

Variable	Univariate			Multivariate		
	<i>t</i>	Standardized β	<i>p</i>	<i>t</i>	Standardized β	<i>p</i>
Total stent length (mm)	3.13	0.165	0.0019	0.83	0.063	0.40
Plaque volume (mm ³)	4.11	0.214	<0.0001	−1.53	−0.266	0.13
True lipid volume (mm ³)	4.86	0.251	<0.0001	2.96	0.462	0.0033
Total stent length (mm)	3.13	0.165	0.0019	0.33	0.025	0.74
Plaque volume (mm ³)	4.11	0.214	<0.0001	−0.37	−0.039	0.71
Estimated lipid volume (mm ³)	5.27	0.271	<0.0001	3.23	0.288	0.0013

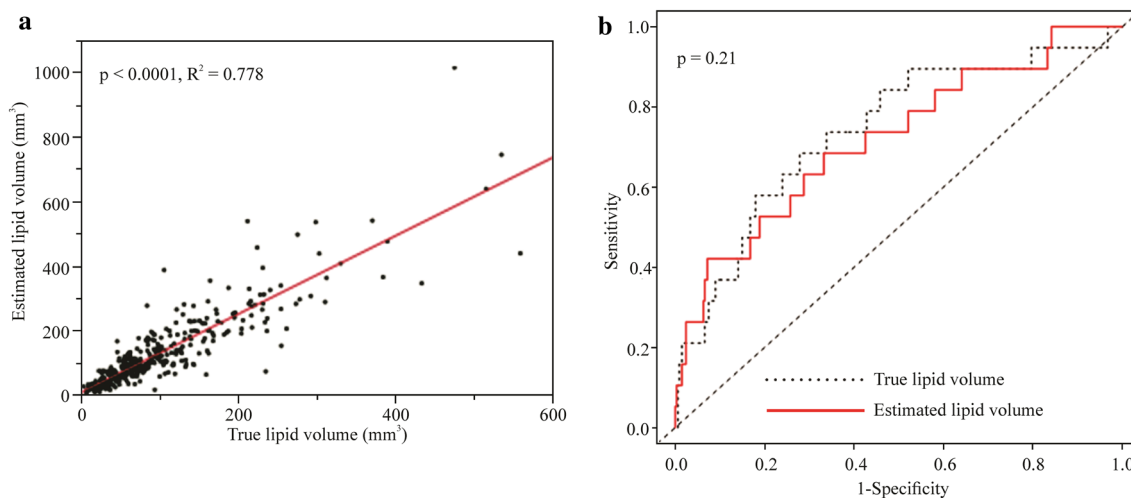


Fig. 3 Comparison between the true and estimated lipid volumes. **a** The estimated lipid volume was strongly correlated with the true lipid volume. **b** Receiver operating characteristic curve for development

of the no-reflow phenomenon with the estimated lipid volume was equivalent to that with the true lipid volume

Table 5 Development of no-reflow phenomenon and cutoff values of true and estimated lipid volume

Number of lesions	No-reflow (+)	No-reflow (–)	
True lipid volume $\geq 117.0 \text{ mm}^3$	13	93	106
True lipid volume $< 117.0 \text{ mm}^3$	6	241	247
	19	334	353
Estimated lipid volume $\geq 132.6 \text{ mm}^3$	13	111	124
Estimated lipid volume $< 132.6 \text{ mm}^3$	6	223	229
	19	334	353

analysis indicated that the NRI for true lipid volume versus estimated lipid volume was 0.45 ($p = 0.043$) and the IDI was 0.018 ($p = 0.45$). AUC values and reclassification analysis suggest that the predictive value of the estimated lipid volume for development of the no-reflow phenomenon was statistically and practically indistinguishable from that of the true lipid volume.

Evaluation of frequency of no-reflow phenomenon using cutoff values

The lesions were separated based on the cutoff values calculated for the true and estimated lipid volumes (Table 5). Among the 19 no-reflow (+) lesions, 13 lesions (68 %) were identified by the estimated lipid volume cutoff value. The cutoff value of the true lipid volume identified the same 13 lesions. In the 124 lesions identified with the estimated lipid volume cutoff value (estimated lipid volume of $\geq 132.6 \text{ mm}^3$), all 13 lesions with no-reflow exhibited a lower incidence of previous MI (23 vs. 52 %, $p = 0.047$), lower hemoglobin levels (12.3 ± 2.1 vs. $13.5 \pm 1.6 \text{ g/dL}$, $p = 0.015$), and a larger true lipid volume (251.0 ± 133.5 vs. $171.6 \pm 89.5 \text{ mm}^3$, $p = 0.0050$). In the group of lesions designated high-risk lesions by the estimated lipid volume cutoff value, the incidence of the no-reflow phenomenon was 10.5 %. Both the true lipid volume and an estimated lipid volume greater than or equal to the cutoff value were associated with an increased risk of the no-reflow phenomenon (odds ratio, 5.61 and 4.35; 95 % CI, 2.15–16.40 and 1.67–12.70; $p = 0.0004$ and 0.0024, respectively).

Discussion

Although the angiographic no-reflow phenomenon rarely occurs during elective PCI, it significantly worsens patient prognosis. IVUS analysis of atherosclerotic lesions can be used to assess the lipid component in target plaques, the main cause of no-reflow in elective PCI. However, it is

difficult to measure the target lesion lipid volume before the PCI procedure. Here, we aimed to design a rapid and reliable method with which to identify coronary lesions at high risk for the no-reflow phenomenon before elective stent implantation using IB-IVUS.

In our study, we examined both transient and persistent no-reflow together. Naturally, the persistent no-reflow phenomenon (final TIMI flow grade of 0–2) leads to a poor prognosis. However, the transient no-reflow phenomenon also causes high in-hospital mortality and a poor long-term prognosis. Transient no-reflow during coronary intervention with grade 3 TIMI flow at completion of the procedure has been associated with increased mortality in previous studies [1, 2]. Additionally, in elective PCI, if no-reflow occurs once, an entirely new ischemic event will be led regardless of whether the no-reflow phenomenon is transient or persistent. Therefore, transient no-reflow during elective PCI should be given close attention and treated in the same way as the persistent no-reflow phenomenon. The incidence of the no-reflow phenomenon in the present study was 5.4 % higher than that in past articles. One reason may be that our study included transient no-reflow. Additionally, with the development of the drug-eluting stent as opposed to the bare-metal stent, the strategy of completely covering a long atherosclerotic plaque has become dominant. However, longer stents have disadvantages with respect to the development of no-reflow because they may allow a greater amount of gruel to leak from the target plaque. Stent length may therefore be one factor accounting for the relatively high no-reflow incidence observed in our study. No significant differences in patient backgrounds were observed between the no-reflow (+) group and no-reflow (–) group. However, hemoglobin levels tended to be lower in patients exhibiting the no-reflow phenomenon than in those who did not; this tendency may reflect that in general, patients with no-reflow were slightly older. In terms of lesion characteristics, Type C lesions, grade 0 TIMI flow, larger vessel size, and larger lipid volume were associated with no-reflow. Type C lesions often have a diffuse atherosclerotic plaque ($>20 \text{ mm}$), and this coincides with the observation that the total stent length for lesions with no-reflow was significantly longer than in lesions without no-reflow. Grade 0 TIMI flow and a larger vessel size as measured with IB-IVUS are also due to a greater atherosclerotic plaque volume and a larger lipid component in the plaques of no-reflow lesions. These results suggest that the no-reflow phenomenon is associated with longer lesion length and positive remodeling of the target vessel and are consistent with previous studies [6, 15, 19]. In the PCI procedures, some differences existed between the no-reflow (+) and no-reflow (–) groups. However, the higher ratio of pre-dilation in the no-reflow (+) group reflects the relative complexity of the target lesions encountered. The low

inflation pressures and long procedural duration in the no-reflow (+) group were likely the results as opposed to the cause of the no-reflow phenomenon.

Integrated backscatter intravascular ultrasound allows for accurate characterization of coronary plaques when compared with histology in autopsied arterial specimens [9, 12] and demonstrates lipid reduction in atherosclerotic plaques with statin therapy [20, 21]. There are two commercial methods for evaluating lesion plaque components using IVUS: IB-IVUS and virtual histology IVUS (VH-IVUS; Volcano Corp, San Diego, CA, USA). Both methods rely on acquired radiofrequency signals from tissue, but adopt different algorithms. In IB-IVUS, a frequency spectrum is constructed using fast Fourier transformation, and radiofrequency signals are analyzed directly. In contrast, in VH-IVUS, a frequency spectrum is constructed using autoregressive analysis of radiofrequency signals, and radiofrequency signals are modified by eight parameters for visualization. Both methods have a high predictive accuracy with respect to lipid components. Furthermore, both methods are reportedly useful in predicting the risk of distal embolization during PCI for acute coronary syndrome [22, 23]. However, a few studies have compared these two methods directly. Okubo et al. [24] compared IB-IVUS and VH-IVUS with histology as the gold standard and declared that IB-IVUS provided higher diagnostic accuracy than VH-IVUS for tissue characterization of coronary plaques. IB-IVUS has revealed a relationship between lipid volume and the development of the no-reflow phenomenon. In patients with acute MI, the amount of plaque was strongly correlated with both transient and persistent no-reflow during stent implantation [16, 25]. In patients with unstable angina undergoing PCI, the no-reflow phenomenon was more likely in plaques with greater volume and a higher lipid ratio [22]. Moreover, vulnerable plaques causing acute coronary syndrome have a greater lipid area than do stable plaques [26]. Leakage of lipid components is an important factor in the development of the no-reflow phenomenon.

Several studies have investigated lipid volume using IB-IVUS in elective stent implantation. Uetani et al. [27] reported a cutoff lipid volume for post-procedural MI of 45.6 mm³ (sensitivity 100.0 %, specificity 67.3 %). In our study, the cutoff lipid volume was 117.0 mm³ (sensitivity 68.4 %, specificity 72.2 %) for the development of the no-reflow phenomenon. This is larger than in the previous study; however, the cutoff value in their study was for post-procedural myocardial injury defined as a troponin T level of >0.3 ng/mL, and the ratio of myocardial injury was 11.4 % in all cases, including cases without no-reflow. In our study, the ratio of angiographic no-reflow was 5.4 %, and the development of no-reflow caused the CK concentration to more obviously increase after PCI.

The difference in these cutoff values may derive from the differences in the population in each study. Nonetheless, analysis of the true lipid volume is useful to identify lesions at high risk for the no-reflow phenomenon because of a strong association between lipid volume and the development of the no-reflow phenomenon. While lesion length and stent length were important factors in the development of no-reflow, the lipid volume data included information on length. In our study, lipid volume was the only predictor among the variables stemming from lesion characteristics. However, this parameter cannot be used immediately before stenting because the analysis is too time-consuming (15–20 min).

We propose measurement of the estimated lipid volume as a rapid and simple technique with which to predict lesions at high risk for the no-reflow phenomenon immediately before PCI. The estimated lipid volume is defined as the lipid area at the MLD site \times total stent length. These two factors are easily measured before stent implantation. According to the ROC analysis, the cutoff estimated lipid volume (132.6 mm³; sensitivity 68.4 %, specificity 66.8 %) for development of the no-reflow phenomenon had a predictive value equivalent to that of the true lipid volume for the prediction of no-reflow. The estimated and true lipid volume cutoffs identified the same lesions for the prediction of no-reflow and identified lesions with a 10 % risk of the no-reflow phenomenon. Baim et al. [28] reported that the incidence of no-reflow in PCI for saphenous vein grafts was <10 % and that distal embolic protection devices reduced the development of no-reflow and prevented major adverse cardiac events. Both the true and estimated lipid volumes might provide clinically relevant tools with which to identify patients who are expected to benefit from distal embolic protection devices. However, the estimated lipid volume is rapidly and reliably measured and can guide decisions regarding stent size, final pressure for stent dilation, intracoronary injection of nicorandil and/or sodium nitroprusside, and use of an embolic protection device. The prevention and/or reduction of no-reflow can improve the patient prognosis after elective PCI.

This retrospective observational study was conducted at a single center with a relatively small number of patients with no-reflow. The mean low-density-lipoprotein cholesterol concentration in the patients of this study was >100 mg/dL, a factor that may have influenced the development of the no-reflow phenomenon. Furthermore, because our method depends on IVUS images of the target lesion, there were some lesions whose morphology prevented assessment: lesions that the IVUS catheter could not cross and lesions with severe calcification. Additional prospective studies with larger sample sizes are needed to validate the conclusions of this study.

Conclusions

The simple and rapid measurement of the estimated lipid volume immediately before stenting in PCI constitutes a reliable predictor of lesions at high risk for the no-reflow phenomenon and may thus optimize the procedure and improve patient prognosis.

Acknowledgments The authors wish to thank Dr. Masaharu Kanazawa for providing helpful suggestions.

Compliance with ethical standards

Ethical approval The investigation conformed to the Declaration of Helsinki. The study was approved by the ethical committee of our Medical Center.

Informed consent Informed consent was obtained from all individual participants included in the study.

Conflict of interest The authors declare that they have no conflict of interest.

References

1. Mehta RH, Harjai KJ, Boura J, Cox D, Stone GW, O'Neill W, Grines CL, Primary Angioplasty in Myocardial Infarction (PAMI) Investigators (2003) Prognostic significance of transient no-reflow during primary percutaneous coronary intervention for ST-elevation acute myocardial infarction. *Am J Cardiol* 92:1445–1447
2. Chan W, Stub D, Clark DJ, Ajani AE, Andrianopoulos N, Brennan AL, New G, Black A, Shaw JA, Reid CM, Dart AM, Duffy SJ, Melbourne Interventional Group Investigators (2012) Usefulness of transient and persistent no-reflow to predict adverse clinical outcomes following percutaneous coronary intervention. *Am J Cardiol* 109:478–485
3. Morishima I, Sone T, Okumura K, Tsuboi H, Kondo J, Mukawa H, Matsui H, Toki Y, Ito T, Hayakawa T (2000) Angiographic no-reflow phenomenon as a predictor of adverse long-term outcome in patients treated with percutaneous transluminal coronary angioplasty for first acute myocardial infarction. *J Am Coll Cardiol* 36:1202–1209
4. Resnic FS, Wainstein M, Lee MK, Behrendt D, Wainstein RV, Ohno-Machado L, Kirshenbaum JM, Rogers CD, Popma JJ, Piana R (2003) No-reflow is an independent predictor of death and myocardial infarction after percutaneous coronary intervention. *Am Heart J* 145:42–46
5. Jinnouchi H, Sakakura K, Wada H, Arao K, Kubo N, Sugawara Y, Funayama H, Momomura S, Ako J (2014) Transient no-reflow following primary percutaneous coronary intervention. *Heart Vessels* 29:429–436
6. Jaffe R, Dick A, Strauss BH (2010) Prevention and treatment of microvascular obstruction-related myocardial injury and coronary no-reflow following percutaneous coronary intervention: a systematic approach. *JACC Cardiovasc Interv* 3:695–704
7. Jaffe R, Charron T, Puley G, Dick A, Strauss BH (2008) Microvascular obstruction and the no-reflow phenomenon after percutaneous coronary intervention. *Circulation* 117:3152–3156
8. Nagai T, Hirano T, Tsunoda M, Hosaka H, Kishino Y, Katayama T, Matsumura K, Miyagawa T, Kohsaka S, Anzai T, Fukuda K, Suzuki M (2013) Left circumflex coronary artery is protected against no-reflow phenomenon following percutaneous coronary intervention for coronary artery disease. *Heart Vessels* 28:559–565
9. Kawasaki M, Takatsu H, Noda T, Ito Y, Kunishima A, Arai M, Nishigaki K, Takemura G, Morita N, Minatoguchi S, Fujiwara H (2001) Noninvasive quantitative tissue characterization and two-dimensional color-coded map of human atherosclerotic lesions using ultrasound integrated backscatter: comparison between histology and integrated backscatter images. *J Am Coll Cardiol* 38:486–492
10. Kawasaki M, Takatsu H, Noda T, Sano K, Ito Y, Hayakawa K, Tsuchiya K, Arai M, Nishigaki K, Takemura G, Minatoguchi S, Fujiwara T, Fujiwara H (2002) In vivo quantitative tissue characterization of human coronary arterial plaques by use of integrated backscatter intravascular ultrasound and comparison with angioscopic findings. *Circulation* 105:2487–2492
11. Okubo M, Kawasaki M, Ishihara Y, Takeyama U, Kubota T, Yamaki T, Ojio S, Nishigaki K, Takemura G, Saio M, Takami T, Minatoguchi S, Fujiwara H (2008) Development of integrated backscatter intravascular ultrasound for tissue characterization of coronary plaques. *Ultrasound Med Biol* 34:655–663
12. Ohota M, Kawasaki M, Ismail TF, Hattori K, Serruys PW, Ozaki Y (2012) A histological and clinical comparison of new and conventional integrated backscatter intravascular ultrasound (IB-IVUS). *Circ J* 76:1678–1686
13. Iwama M, Tanaka S, Noda T, Segawa T, Kawasaki M, Nishigaki K, Minagawa T, Watanabe S, Minatoguchi S (2014) Impact of tissue characteristics on luminal narrowing of mild angiographic coronary stenosis: assessment of integrated backscatter intravascular ultrasound. *Heart Vessels* 29:750–760
14. Kumagai S, Takashima H, Waseda K, Ando H, Suzuki A, Uetani T, Harada K, Yoshida T, Kunimura A, Shimbo Y, Kitagawa K, Harada K, Ishii H, Yoshikawa D, Matsubara T, Murohara T, Amano T (2014) Prognostic impact of lipid contents on the target lesion in patients with drug eluting stent implantation. *Heart Vessels* 29:761–768
15. Watanabe T, Nanto S, Uematsu M, Ohara T, Morozumi T, Kotani J, Nishio M, Awata M, Nagata S, Hori M (2003) Prediction of no-reflow phenomenon after successful percutaneous coronary intervention in patients with acute myocardial infarction: intravascular ultrasound findings. *Circ J* 67:667–671
16. Wu X, Mintz GS, Xu K, Lansky AJ, Witzensbichler B, Guagliumi G, Brodie B, Kellett MA Jr, Dressler O, Parise H, Mehran R, Stone GW, Maehara A (2011) The relationship between attenuated plaque identified by intravascular ultrasound and no-reflow after stenting in acute myocardial infarction: the HORIZONS-AMI (harmonizing outcomes with revascularization and stents in acute myocardial infarction) trial. *JACC Cardiovasc Interv* 4:495–502
17. Utsunomiya M, Hara H, Sugi K, Nakamura M (2011) Relationship between tissue characterisations with 40 MHz intravascular ultrasound imaging and slow flow during coronary intervention. *EuroIntervention* 7:340–346
18. Mintz GS, Nissen SE, Anderson WD, Bailey SR, Erbel R, Fitzgerald PJ, Pinto FJ, Rosenfield K, Siegel RJ, Tuzcu EM, Yock PG (2001) American college of cardiology clinical expert consensus document on standards for acquisition, measurement and reporting of intravascular ultrasound studies (IVUS). A report of the American college of cardiology task force on clinical expert consensus documents. *J Am Coll Cardiol* 37:1478–1492
19. Takeuchi H, Morino Y, Matsukage T, Masuda N, Kawamura Y, Kasai S, Hashida T, Fujibayashi D, Tanabe T, Ikari Y (2009) Impact of vascular remodeling on the coronary plaque composition: an investigation with in vivo tissue characterization using integrated backscatter-intravascular ultrasound. *Atherosclerosis* 202:476–482

20. Kawasaki M, Sano K, Okubo M, Yokoyama H, Ito Y, Murata I, Tsuchiya K, Minatoguchi S, Zhou X, Fujita H, Fujiwara H (2005) Volumetric quantitative analysis of tissue characteristics of coronary plaques after statin therapy using three-dimensional integrated backscatter intravascular ultrasound. *J Am Coll Cardiol* 45:1946–1953
21. Hattori K, Ozaki Y, Ismail TF, Okumura M, Naruse H, Kan S, Ishikawa M, Kawai T, Ohta M, Kawai H, Hashimoto T, Takagi Y, Ishii J, Serruys PW, Narula J (2012) Impact of statin therapy on plaque characteristics as assessed by serial OCT, grayscale and integrated backscatter-IVUS. *JACC Cardiovasc Imaging* 5:169–177
22. Shibuya M, Okamura A, Hao H, Date M, Higuchi Y, Nagai H, Ozawa M, Masuyama T, Iwakura K, Fujii K (2013) Prediction of distal embolization during percutaneous coronary intervention for unstable plaques with grayscale and integrated backscatter intravascular ultrasound. *Catheter Cardiovasc Interv* 81:E165–E172
23. Kawaguchi R, Oshima S, Jingu M, Tsurugaya H, Toyama T, Hoshizaki H, Taniguchi K (2007) Usefulness of virtual histology intravascular ultrasound to predict distal embolization for ST-segment elevation myocardial infarction. *J Am Coll Cardiol* 50:1641–1646
24. Okubo M, Kawasaki M, Ishihara Y, Takeyama U, Yasuda S, Kubota T, Tanaka S, Yamaki T, Ojio S, Nishigaki K, Takemura G, Saio M, Takami T, Fujiwara H, Minatoguchi S (2008) Tissue characterization of coronary plaques: comparison of integrated backscatter intravascular ultrasound with virtual histology intravascular ultrasound. *Circ J* 72:1631–1639
25. Iijima R, Shinji H, Ikeda N, Itaya H, Makino K, Funatsu A, Yokouchi I, Komatsu H, Ito N, Nuruki H, Nakajima R, Nakamura M (2006) Comparison of coronary arterial finding by intravascular ultrasound in patients with “transient no-reflow” versus “reflow” during percutaneous coronary intervention in acute coronary syndrome. *Am J Cardiol* 97:29–33
26. Sano K, Kawasaki M, Ishihara Y, Okubo M, Tsuchiya K, Nishigaki K, Zhou X, Minatoguchi S, Fujita H, Fujiwara H (2006) Assessment of vulnerable plaques causing acute coronary syndrome using integrated backscatter intravascular ultrasound. *J Am Coll Cardiol* 47:734–741
27. Uetani T, Amano T, Ando H, Yokoi K, Arai K, Kato M, Marui N, Nanki M, Matsubara T, Ishii H, Izawa H, Murohara T (2008) The correlation between lipid volume in the target lesion, measured by integrated backscatter intravascular ultrasound, and post-procedural myocardial infarction in patients with elective stent implantation. *Eur Heart J* 29:1714–1720
28. Baim DS, Wahr D, George B, Leon MB, Greenberg J, Cutlip DE, Kaya U, Popma JJ, Ho KK, Kuntz RE (2002) Randomized trial of a distal embolic protection device during percutaneous intervention of saphenous vein aorto-coronary bypass grafts. *Circulation* 105:1285–1290